HGT

Host Immune Responses after Suprachoroidal Delivery of AAV8 in Nonhuman Primate Eyes

Sook Hyun Chung,[1] Iris Natalie Mollhoff,[1] Alaknanda Mishra,[2] Tzu-Ni Sin,[1] Taylor Ngo,[1] Thomas Ciulla,[3] Paul Sieving,[1] Sara M. Thomasy,[1,4] and Glenn Yiu[1,*]

Departments of [1]Ophthalmology and Vision Science and [2]Cell Biology and Human Anatomy, University of California Davis, Davis, California, USA; [3]Clearside Biomedical, Inc., Alpharetta, Georgia, USA; [4]Department of Surgical and Radiological Sciences, School of Veterinary Medicine, University of California Davis, Davis, California, USA.

The suprachoroid is a potential space located between the sclera and choroid of the eye, which provides a novel route for ocular drug or viral vector delivery. Suprachoroidal injection of adeno-associated virus (AAV)8 using transscleral microneedles enables widespread transgene expression in eyes of nonhuman primates, but may cause intraocular inflammation. We characterized the host humoral and cellular immune responses after suprachoroidal delivery of AAV8 expressing green fluorescent protein (GFP) in rhesus macaques, and found that it can induce mild chorioretinitis that resolves after systemic corticosteroid administration, with recovery of photoreceptor morphology, but persistent immune cell infiltration after 3 months, corresponding to a loss of GFP expression from retinal pigment epithelial cells, but persistent expression in scleral fibroblasts. Suprachoroidal AAV8 triggered B cell and T cell responses against GFP, but only mild antibody responses to the viral capsid compared to intravitreal injections of the same vector and dose. Systemic biodistribution studies showed lower AAV8 levels in liver and spleen after suprachoroidal injection compared with intravitreal delivery. Our findings suggest that suprachoroidal AAV8 primarily triggers host immune responses to GFP, likely due to sustained transgene expression in scleral fibroblasts outside the blood–retinal barrier, but elicits less humoral immune reactivity to the viral capsid than intravitreal delivery due to lower egress into systemic circulation. As GFP is not native to primates and not a clinically relevant transgene, suprachoroidal AAV delivery of human transgenes may have significant translational potential for retinal gene therapy.

Keywords: suprachoroidal injection, AAV, ocular gene therapy, host immune response

INTRODUCTION

THE FIRST APPROVED ocular gene therapy for treating biallelic RPE65 mutation-associated retinal dystrophy, Leber's Congenital Amaurosis, has generated much enthusiasm for the use of adeno-associated viruses (AAVs) as vectors for retinal gene delivery.[1,2–6] Recombinant AAVs are highly effective vectors for gene delivery due to their ability to transduce a wide variety of retinal cell types and relative safety, given their nonpathogenic and nonintegrating nature.[7] However, although AAV vectors are much less immunogenic than adenoviruses, host immune responses triggered by the viral vector or transgene product can limit the effectiveness of the treatment.[8,9]

Humoral immune responses from neutralizing antibodies (NAbs) produced by B cells can inhibit vector transduction. These antibodies may arise from prior exposure to wild-type AAV causing pre-existing immunity, or be triggered by therapeutic vector administration, which prevents or suppresses further transduction.[10–13] Also, cell-mediated immune responses from cytokine-secreting T cells can directly destroy transduced cells.[14] Together, host humoral and cellular immune responses contribute to eliminating vectors and transduced cells, thus limiting the therapeutic effect.

Although the eye has been considered to be an immunologically protected space,[15] the immunogenicity of AAV-mediated gene transfer in the eye varies with the route of administration. Subretinal injections, which entail a needle puncture through the neurosensory retina, enable efficient transduction of multiple cell types, including photoreceptors and the underlying retinal pigment

*Correspondence: Dr. Glenn Yiu, Department of Ophthalmology and Vision Science, University of California Davis, 4860 Y Street, Suite 2400, Sacramento, CA 95817, USA. E-mail: gyiu@ucdavis.edu

DOI: 10.1089/hum.2020.281

epithelium (RPE), and trigger minimal humoral immune responses.[16,17] However, the procedure requires complex vitrectomy surgery and the therapeutic effect is limited to the area of the injected fluid bleb.

Intravitreal injections can be easily performed in an outpatient clinical setting, and newer generations of AAV can overcome the internal limiting membrane barrier to transduce deeper retinal layers.[18,19] However, unlike subretinal injections, intravitreal delivery triggers more pronounced humoral and cellular responses against the AAV capsid, occasionally to levels matching systemic administration.[13,20]

We and others have recently described a novel mode of ocular gene delivery by injecting AAV into the suprachoroidal space, which is located between the scleral wall and the choroidal vasculature of the eye.[21,22] Although this potential space is barely detectable under physiologic conditions,[23,24] suprachoroidal injection of compounds using transscleral microneedles expands the suprachoroidal space as seen on *in vivo* imaging,[25,26] enabling targeted drug delivery to retinal and choroidal tissues, while minimizing adverse effects on anterior segment structures.[27–31] Suprachoroidal injection of a triamcinolone acetonide suspension using these microneedles has been effective in treating macular edema from noninfectious uveitis in human clinical trials.[32]

Using nonhuman primates (NHPs), we previously found that suprachoroidal injection of AAV8 using transscleral microneedles enables widespread, peripheral transduction of mostly RPE cells. By contrast, subretinal injection of AAV8 transduced outer retinal cells, including photoreceptors and RPEs, but was limited to the injection site.[21] Since the suprachoroidal space is located outside the blood–retinal barrier, we also investigated the inflammatory response in retinal and choroidal tissues, and found a greater degree of local immune cell infiltration after suprachoroidal delivery of AAV8 compared with subretinal or intravitreal injections. Interestingly, we found that intravitreal AAV8 triggered more serum NAbs than the other modes of injection, likely due to differences in the pharmacokinetics and biodistribution of the different modes of ocular AAV delivery.

In this ancillary analysis of our prior study,[21] we explore in detail the host humoral and cellular immune responses to suprachoroidal AAV8 in these rhesus macaques. Like humans, NHPs are natural hosts for wild-type AAV and develop immune conversions to subclinical infection, making them an excellent animal model for predicting host immune responses to AAV vectors in humans.

We found that suprachoroidal injection of AAV8 expressing green fluorescent protein (GFP) can elicit a transient chorioretinitis that clinically resolves after systemic corticosteroid administration, with recovery of photoreceptor morphology, despite some persistence of immune cell infiltration over 3 months. Suprachoroidal injections trigger both B cell and T cell responses against the GFP transgene product, whereas the response against AAV8 capsid was minimal compared with intravitreal injections. Systemic biodistribution assays showed limited presence of the AAV8 in the liver and spleen after suprachoroidal injections compared with intravitreal delivery. As suprachoroidal injection of AAV is currently under evaluation for retinal gene therapy in human clinical trials, our results provide an important, clinically relevant, and unique exploration of host immune responses from viral gene delivery to different ocular compartments surrounding the blood–retinal barrier.

METHODS

AAV8 production and intraocular injection

The AAV cis construct, which expresses enhanced GFP under a cytomegalovirus (CMV) promoter, was packaged into AAV8 capsid and purified by the UC Davis NEI Vision Molecular Construct and Packaging Core. After animal sedation, eyes were sterilely prepped with 1% povidone-iodine and flushed with sterile saline, followed by placement of an eyelid speculum. For transscleral microneedle injections, a 700-μm-long 30-gauge microneedle (Clearside Biomedical) was inserted through the conjunctiva and sclera at 4 or 10 mm posterior to the corneal limbus to inject into the superotemporal quadrant (single 100 μL injection) of left eyes and both superotemporal and inferonasal quadrants (two 50 μL injections) of right eyes.

For intravitreal injections, a 0.5-inch-long 30-gauge needle (BD Biosciences) was inserted through the pars plana, 4 mm posterior to the limbus, in the inferotemporal quadrant (single 100 μL injection) of both eyes. The viral concentrations are reported in Supplementary Table S1. Intraocular pressure (IOP) was measured following intraocular injections, and an anterior chamber tap was performed using a 30-gauge needle to remove aqueous until the IOP was normalized.

Rhesus 02, which received high-dose suprachoroidal AAV8, showed signs of ocular irritation and was found to have mild AC cells at 2 weeks after the injection, and was treated with oral prednisone (1 mg/kg) for 2 weeks. In Rhesus 03, 04, and 05, a 40 mg periorbital subtenon injection of triamcinolone acetonide suspension (Kenalog-40, Bristol-Myers-Squibb) was also given in the superotemporal quadrant at the request of the veterinarian to prevent uveitis.

Imaging

All animals underwent scanning laser ophthalmoscopy (SLO) and spectral domain-optical coherence tomography (SD-OCT) imaging using the Spectralis HRA+OCT device (Heidelberg Engineering, Heidelberg, Germany) before and at 1 week, 1 month, and 2 or 3 months after AAV injections. Confocal SLO was used to capture $55° \times 55°$ or $30° \times 30°$ fluorescence images using 488 nm excitation light and a long-pass barrier filter starting at 500 nm. Images were captured from the central macula

and from the peripheral retina by manually steering the Spectralis device. Due to the facial contour of these animals, the superior quadrants could be seen on live visualization, but was difficult to capture at sufficient quality for image montage.

SD-OCT was performed alongside infrared reflectance images using an 820 nm diode laser to capture $30° \times 5°$ SD-OCT raster scans with 1536 A-scans per B-scan and 234 μm spacing between B-scans, in high-resolution mode. SD-OCT scans were captured from the central macula and in regions of visible GFP fluorescence, especially near the junction between transduced and untransduced tissues. Twenty-five scans were averaged for each B-scan, using the Heidelberg eye tracking Automatic Real-Time (ART) software. Animals also underwent color fundus photography (CF-1; Canon) for documentation of clinical examination findings when possible.

Peripheral blood mononuclear cell and splenocyte collection

For peripheral blood mononuclear cell (PBMC) isolation, anticoagulated blood was diluted in phosphate-buffered saline (PBS), layered over Ficoll Paque Premium (17544202; GE Healthcare), and centrifuged for 30 min at $800 \times g$. The PBMC fraction was transferred to PBS and centrifuged again, followed by lysis of red blood cells using Ammonium-Chloride-Potassium (ACK) lysis buffer (A1049201; Gibco), washing with Roswell Park Memorial Institute (RPMI) buffer, and resuspension in 10% dimethyl sulfoxide (DMSO) in heat-inactivated fetal bovine saline (FBS). For splenocyte collection, spleen tissues were homogenized in sterile PBS, passed through a cell strainer, centrifuged, then resuspended in ACK lysis buffer, washed with PBS, and resuspended in 10% DMSO in FBS.

Binding antibody assay

Binding antibody assays were performed to detect antibodies against GFP and AAV capsid in NHP sera as described previously.[33] For anti-AAV8 antibody detection, a sandwich-ELISA kit designed for AAV8 titration was used (PRAAV8; Progen). Briefly, microtiter strips with AAV8-specific antibodies were incubated with AAV8 particles (2×10^{12} vg/mL) overnight at 4°C, blocked with 5% milk in PBS, and then incubated with macaque sera (1:1,000 dilution) at 37°C for 2 h. After washing, the strips were incubated with horse radish peroxidase (HRP)-conjugated anti-rhesus secondary antibodies (1:2000; 6200-50, Southern Biotech) for two additional hours at room temperature, incubated with 3,3′,5,5′-tetramethylbenzidine (0410-01; Southern Biotech), stopped with a stopping solution (0412-01; Southern Biotech), and then read with a plate reader (N16612; Fisher Scientific accuSkan FC) with 450 nm absorbance.

For detecting anti-GFP antibodies, a 96-well plate was coated with enhanced GFP protein (4999-100; BioVision, 5 μg/mL) overnight at 4°C, blocked with 5% nonfat milk in PBS, and then incubated with diluted serum samples (1:5,000) at 37°C for 2 h, followed by detection with HRP-conjugated anti-rhesus immunoglobulin G as described above. Commercial anti-AAV8 (1:100; 610160S, Progen) and anti-GFP (1:1000; ab6556, Abcam) antibodies were used as positive controls, and all values were determined from triplicates. The antibodies were calculated against a standard curve and normalized with total protein.

Enzyme-linked immune absorbent spot

Enzyme-linked immune absorbent spot (ELISpot) assays to detect interferon gamma (IFN-γ)-secreting cells from PBMCs were performed with a commercial kit according to the manufacturer's instruction (CT121; U-CyTech). Briefly, a 96-well polyvinylidene fluoride membrane-bottomed plate was activated with 70% ethanol and coated with anti-IFN-γ antibodies overnight at 4°C. After washing and blocking, PBMCs were seeded at 4×10^5 cells per well in RPMI-160 media containing a mix of 182 AAV8 capsid or enhanced GFP peptides (15mers and 11 overlaps, 4 ng/μL, JPT, PM-AAV8-CP, and PM-EGFP) for 48 h. We incubated the cells with phorbol 12-myristate 13-acetate (PMA, 80 nM) and ionomycin (1.3 μM) for positive control, and DMSO (0.05%) for negative control. After removing the cells, the plate was incubated with biotinylated detection antibody for 2 h followed by streptavidin-HRP and 3-amino-9-ethylcarbazole (AEC) substrate. Spots were counted and normalized with negative control. Spot-forming unit (SFU) was calculated from triplicates converted to SFU per 10^6 cells.

Quantitative polymerase chain reaction

Systemic biodistribution assays were performed using quantitative polymerase chain reaction (qPCR) with SYBR Green. Liver, spleen, and kidney samples were collected at necropsy, and genomic DNA (gDNA) was extracted using a commercial kit following the manufacturer's instruction (69504; Qiagen). For qPCR, each reaction contained 10 ng of gDNA with SYBR Green qPCR master mix (Invitrogen) and forward and reverse primers. qPCR cycling was 95° for 10 min, and 40 cycles of 95° for 10 min, 60° for 1 min, and melting curve analysis was performed for primer dimers. Copy number of GFP transgene was calculated against standard curve, and rhesus beta actin primer set was used as an internal control in a separate reaction.

The primer sets used in this study are enhanced GFP forward 5′-AGATCCGCCACAACATCGAGG-3′, GFP reverse 5′-AGCAGGACCATGTGATCGC-3′, beta-actin forward 5′-GGGCCGGACTCGTCATAC-3′, and beta-actin reverse 5′-CCTGGCACCCAGCACAAT-3′. The limit of detection was 162 copies/μg DNA.

Immunohistochemistry

Immunohistochemistry was performed as described previously.[21] Posterior eye cups were fixed with 4%

paraformaldehyde for 2 h after removal of anterior segments lens and vitreous. After washing with PBS, tissues were cryoprotected with 30% sucrose overnight, then embedded, and cryosectioned at 18 μm. Frozen sections were carefully selected based on the native GFP expression, and washed with PBS, blocked with 10% normal donkey serum for 30 min, and then incubated in primary antibody for 1–2 h at room temperature, followed by Alexa Fluor-conjugated secondary antibodies. Primary antibodies include ionized calcium-binding adaptor-1 (IBA-1) (1:100; AB10558, Wako), glial fibrillary acidic protein (GFAP) (1:200; Z0334, Dako), and CD45 (552566; BD, 2.5 μg/mL).

Flow cytometry

For flow cytometry, 0.5×10^6 PBMCs or splenocytes per well were plated in duplicate in 96-well plates in RPMI supplemented with 10% FBS for 24 h. The cells were stimulated with AAV8 peptide (4 ng/μL, JPT and PM-AAV8-CP), GFP peptide (4 ng/μL, JPT and PM-EGFP), cRPMI alone (unstimulated), or PMA (80 nM)-ionomycin (1.3 μM) (positive control). Cultures were incubated at 37°C for 48 h, washed with PBS, and stained for flow cytometric analysis. The cells were incubated with 50 μL of an antibody cocktail for CD8 (Q10055; Thermo Fisher), HLADR (307656; BioLegend), CD19 (302239; BioLegend), CD27 (302824; Biolegend), and CD38 (100825; Labcome) for 30 min at room temperature in the dark, followed by two washes with fluorescence-activated cell sorting (FACS) buffer (PBS +1% FBS), and resuspended in 300 μL of FACS buffer for analysis. The data were acquired within an hour on a BD FACS LSR II flow cytometer (Beckman Coulter Life Sciences, USA).

Study approval

The California National Primate Research Center (CNPRC) is accredited by the Association for Assessment and Accreditation of Laboratory Animal Care (AAALAC) International. All studies using rhesus macaques (*Macaca mulatta*) followed the guidelines of the Association for Research in Vision and Ophthalmology (ARVO) Statement for the Use of Animals in Ophthalmic and Vision Research, and complied with the National Institutes of Health (NIH) Guide for the Care and Use of Laboratory Animals. All procedures were conducted under protocols approved by the University of California, Davis Institutional Animal Care and Use Committee (IACUC).

RESULTS

Study design and clinical course

Our prior experiments to evaluate the transduction efficacy, pattern, durability, and cell-type specificity of suprachoroidal AAV8 injections in rhesus macaques using transscleral microneedles have been previously described.[21] Briefly, we identified five animals between age 4–10 years with no pre-existing NAbs against AAV8, and injected both eyes with NHP-grade AAV8 that expresses enhanced GFP under a CMV promoter at 7×10^{11} vg/eye (low dose) or 7×10^{12} vg/eye (high dose), using either a 700-μm-long 30-gauge microneedle (Clearside Biomedical, Alpharetta, GA, USA) for suprachoroidal or transscleral subretinal injection or a 0.5-inch-long 30-gauge conventional needle for intravitreal injection (Supplementary Table S1). Of these, two animals received suprachoroidal AAV8 in both eyes (Rhesus 01 with 7×10^{11} vg/eye and Rhesus 02 with 7×10^{12} vg/eye), two animals (Rhesus 03 and 04) received suprachoroidal injection of AAV8 in one eye (7×10^{12} vg/eye) and subretinal delivery of AAV8 in the contralateral eye (7×10^{12} vg/eye), and the last animal (Rhesus 05) received intravitreal injection of AAV8 in both eyes (7×10^{12} vg/eye).

After 1 month, suprachoroidal delivery of high-dose AAV8 produced diffuse, peripheral, and circumferential GFP fluorescence with a punctate pattern of expression (Fig. 1A). By comparison, subretinal AAV8 resulted in a focal area of intense GFP expression (Fig. 1B), while intravitreal AAV8 only produced a small peripapillary area of faint expression at the same high dose (Fig. 1C). Suprachoroidal delivery of low-dose AAV8 (7×10^{11} vg/eye) did not produce any detectable transgene expression on fundus fluorescence imaging.

Although most of the animals did not exhibit significant anterior chamber (AC) or vitreous inflammation throughout the study, Rhesus 02 developed mild 2+ AC cell based on Standardization of Uveitis Nomenclature criteria at 2 weeks, requiring treatment with oral prednisone (1 mg/kg) for 2 weeks with subsequent resolution of the AC cell by month 1. At 1 month, this animal also demonstrated a peripheral chorioretinitis with small, punctate spots (Fig. 1D), some perivascular sheathing (Fig. 1E), and radial retinal striae in the macular region without significant macular edema (Fig. 1F), which all appeared resolved by month 3 (Fig. 1G–I). SD-OCT imaging showed fine, hyperreflective foci in the vitreous and retinal surface at 1 month (Fig. 1J), indicating subclinical vitritis not readily seen on fundoscopic examination, which also resolved after 3 months (Fig. 1K). We did not note significant vitreous cell in the peripheral regions of the transduced retina in Rhesus 02, or in any other animals after suprachoroidal delivery of AAV (Fig. 1L).

Eyes that received subretinal AAV8 showed localized vascular dilation and perivascular hyperreflective foci in the vitreous in the most intense regions of GFP expression (Fig. 1M, O), indicating localized vasculitis and subclinical vitritis in these animals. Eyes that received intravitreal injection of AAV8 showed no detectable vitritis, chorioretinitis, or vasculitis, even in the small peripapillary region of transduction (Fig. 1N, P). Thus, suprachoroidal injection of AAV8 may trigger an anterior uveitis,

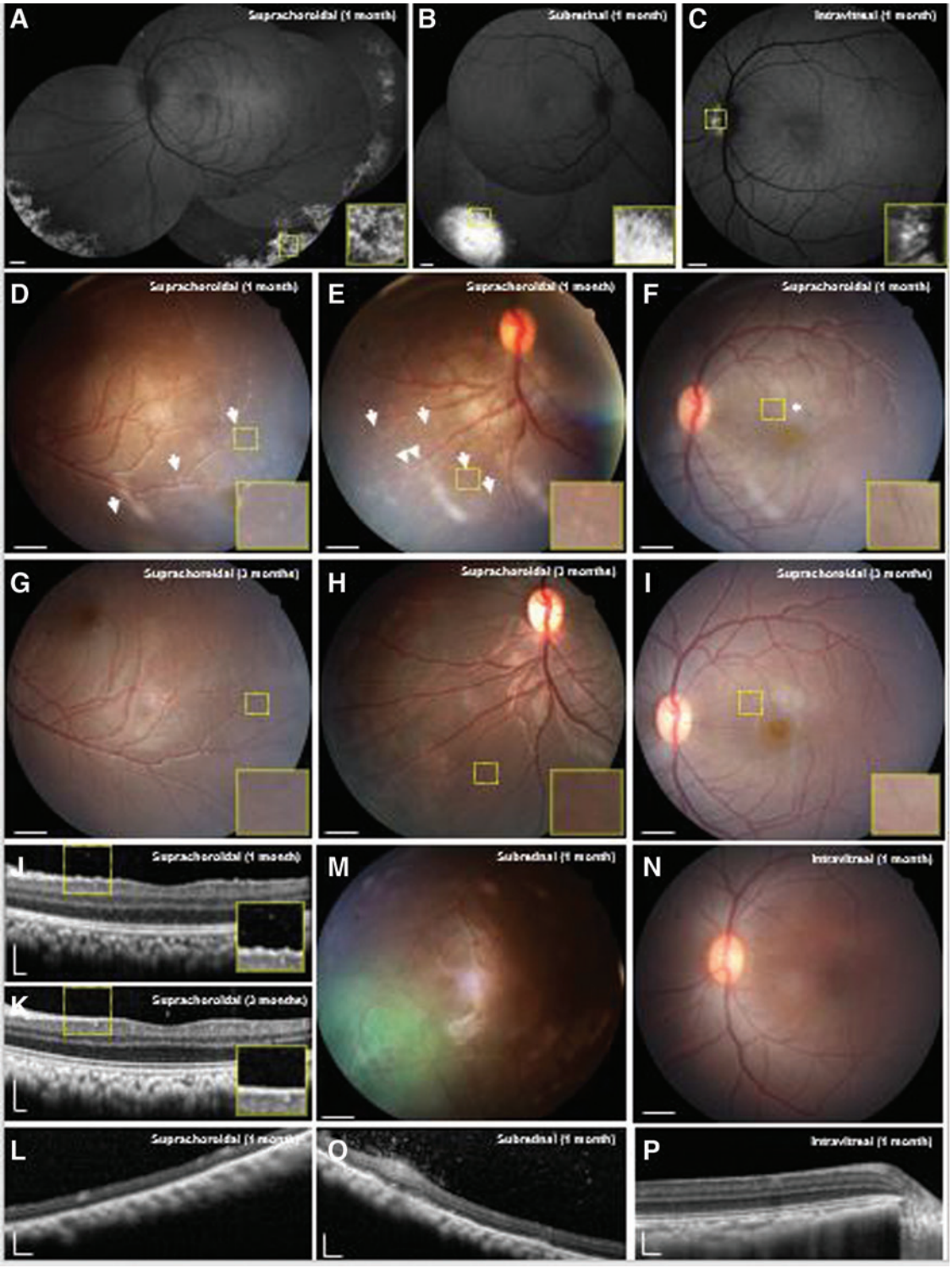

Figure 1. Multimodal ocular imaging after suprachoroidal, subretinal, or intravitreal injections of AAV8 to express enhanced GFP in NHP eyes. **(A–C)** Representative SLO montages and magnified *insets* of the *yellow*-dashed regions show different patterns of GFP transgene expression at 1 month after suprachoroidal, subretinal, and intravitreal AAV delivery. **(D–I)** Representative color fundus photographs and magnified *insets* demonstrate punctate spots (*arrows*), perivascular sheathing (*arrowheads*), and radial macular striae (*asterisk*) that are observed after suprachoroidal AAV8 injections at 1 month **(D–F)**, but resolved by 3 months with some perivascular sheen, but no clear perivascular sheathing **(G–I)**, consistent with a transient chorioretinitis and vasculitis. **(J, L)** Representative SD-OCT images and magnified *insets* of the *yellow-dashed* regions reveal hyperreflective foci seen after suprachoroidal AAV8 at 1 month, but not at 3 months or in peripheral retina. **(M, N)** Fundus photographs of macaque eyes demonstrate GFP fluorescence after subretinal AAV8, and no clear inflammation after subretinal or intravitreal AAV8. **(O, P)** SD-OCT images showed that subretinal AAV8 also induced cellular extravasation from retinal vessels suggestive of a localized vasculitis, but not after intravitreal injections. Scale bars, 1 mm for SLO images and fundus photos; 200 μm for SD-OCT images. AAV, adeno-associated virus; GFP, green fluorescent protein; NHP, nonhuman primate; SD-OCT, spectral domain-optical coherence tomography; SLO, scanning laser ophthalmoscopy. Color images are available online.

peripheral chorioretinitis, and mild vitritis that resolved with oral corticosteroid treatment over 2 weeks. Subretinal AAV8 can also trigger mild, localized vasculitis and vitritis in the area of transduction, while intravitreal AAV8 exhibited poor transduction, but showed no detectable intraocular inflammation.

Local inflammatory responses after suprachoroidal AAV8

We previously found that suprachoroidal AAV8 injection elicited greater local infiltration of inflammatory cells than transscleral subretinal or intravitreal injections at 1 month postinjection.[21] In this study, we further characterize the local inflammation using immunohistochemistry at 2 and 3 months after suprachoroidal AAV8 delivery (Fig. 2). GFP transgene expression was detectable in both RPE and scleral tissues at 1 month, but only persisted in the sclera at months 2 and 3, appearing mostly in spindle-shaped cells that resemble scleral fibroblasts. The GFP expression in the sclera was not visible on live fundus imaging, likely due to blockage of the fluorescence by the dark pigmented RPE and uvea in rhesus macaques.[34]

Local infiltration of Iba1+ microglia and macrophages (Figs. 2A–E), CD45+ leukocytes (Figs. 2F–J), and CD8+ cytotoxic T cells (Fig. 2K–O), as well as reactive gliosis as shown by GFAP staining (Fig. 2P–T), were detected through month 3 compared to uninjected control animals. Interestingly, the outer retinal layers and RPE architecture appeared partly restored at month 3 in the animal that received systemic corticosteroids (Fig. 2U–Y). The animal that received low-dose suprachoroidal AAV8 injections also demonstrated GFP expression in the sclera, and exhibited a similar degree of local inflammatory responses at month 3 (Fig. 2D, I, N, S, and X).

Humoral immune responses after suprachoroidal AAV8

To evaluate humoral immune response from B cells, we employed a sandwich enzyme-linked immunosorbent assay (ELISA) to measure serum binding antibodies against the AAV8 capsid or GFP transgene product after suprachoroidal or intravitreal delivery of the AAV8 vector (Fig. 3A, B). Most of the animals that received suprachoroidal AAV8 developed minimal antibody responses against the viral capsid, whereas the animal that received intravitreal AAV8 exhibited higher anti-AAV8 antibody levels within 1 month (Fig. 3A). These results are consistent with our prior study that demonstrated higher concentrations of serum NAbs from intravitreal than suprachoroidal or subretinal AAV8 as measured using an *in vitro* transduction inhibition assay.[21] By contrast, only animals that received suprachoroidal AAV8 developed anti-GFP antibodies, which reached the highest levels at month 3, while the animal that received only intravitreal AAV8 did not (Fig. 3B).

As Rhesus 02 received high-dose suprachoroidal AAV8 in both eyes, we further validated the humoral response to GFP by performing flow cytometry on PBMCs collected from the serum of this animal, and found expansion of GFP-responsive plasma B cells (CD19–, CD27+, CD38+, and HLADRlow) after suprachoroidal AAV8 injection (Fig. 3C and Supplementary Fig. S1), which likely accounts for the greater production of systemic anti-GFP antibodies. Interestingly, the animal that received low-dose AAV8 (Rhesus 01) also developed similar concentrations of anti-GFP antibodies, likely due to the presence of GFP expression in the sclera of both eyes through month 3 (Fig. 3B). These findings suggest that although intravitreal AAV8 produces an earlier and more robust humoral response to the viral capsid, suprachoroidal delivery triggers greater antibody responses to GFP, possibly due to exposure of GFP-expressing scleral fibroblasts to systemic immune surveillance, given their location outside the blood–retinal barrier.

Cell-mediated immune responses after suprachoroidal AAV8

We next explored cell-mediated immune responses to suprachoroidal AAV8 using ELISpot assays to detect IFN-γ-producing T cells against AAV8 or GFP in PBMCs collected throughout the study and in splenocytes collected at the time of necropsy (Fig. 4). None of the animals showed appreciable T cell responses to the AAV8 capsid with the exception of Rhesus 01, which appeared to have pre-existing T cell responses to AAV8 before injection (Fig. 4A), despite not having anti-AAV8 antibodies (Fig. 3A) or NAbs at baseline.[21]

Similar to the humoral immune responses, suprachoroidal AAV8 also triggered T cell responses to GFP beginning as early as 1 month after injection, particularly in animals that received suprachoroidal injections in both eyes (Fig. 4B). Using splenocytes collected at necropsies, we found suprachoroidal AAV8 injection triggered greater T cell responses to the GFP transgene product than to the viral vector (Fig. 4C–D). Our results suggest that both humoral and cellular immunity against the GFP transgene corresponded more with the route of delivery than the vector dose.

Systemic biodistribution of suprachoroidal AAV8

To evaluate systemic biodistribution after suprachoroidal AAV8 delivery, we performed qPCR to detect the GFP transgene sequence in gDNA from peripheral organs, including kidney, liver, and spleen. The highest genome copies were detected in the spleen, followed by the liver, and was undetectable in the kidney (Fig. 5). Interestingly, the animal that received intravitreal injections of AAV8 in both eyes (Rhesus 05) showed much higher genome copies of the vector in the spleen and liver, compared to animals that received suprachoroidal AAV8 in both eyes (Rhesus 01 and 02) or suprachoroidal and subretinal AAV8 in

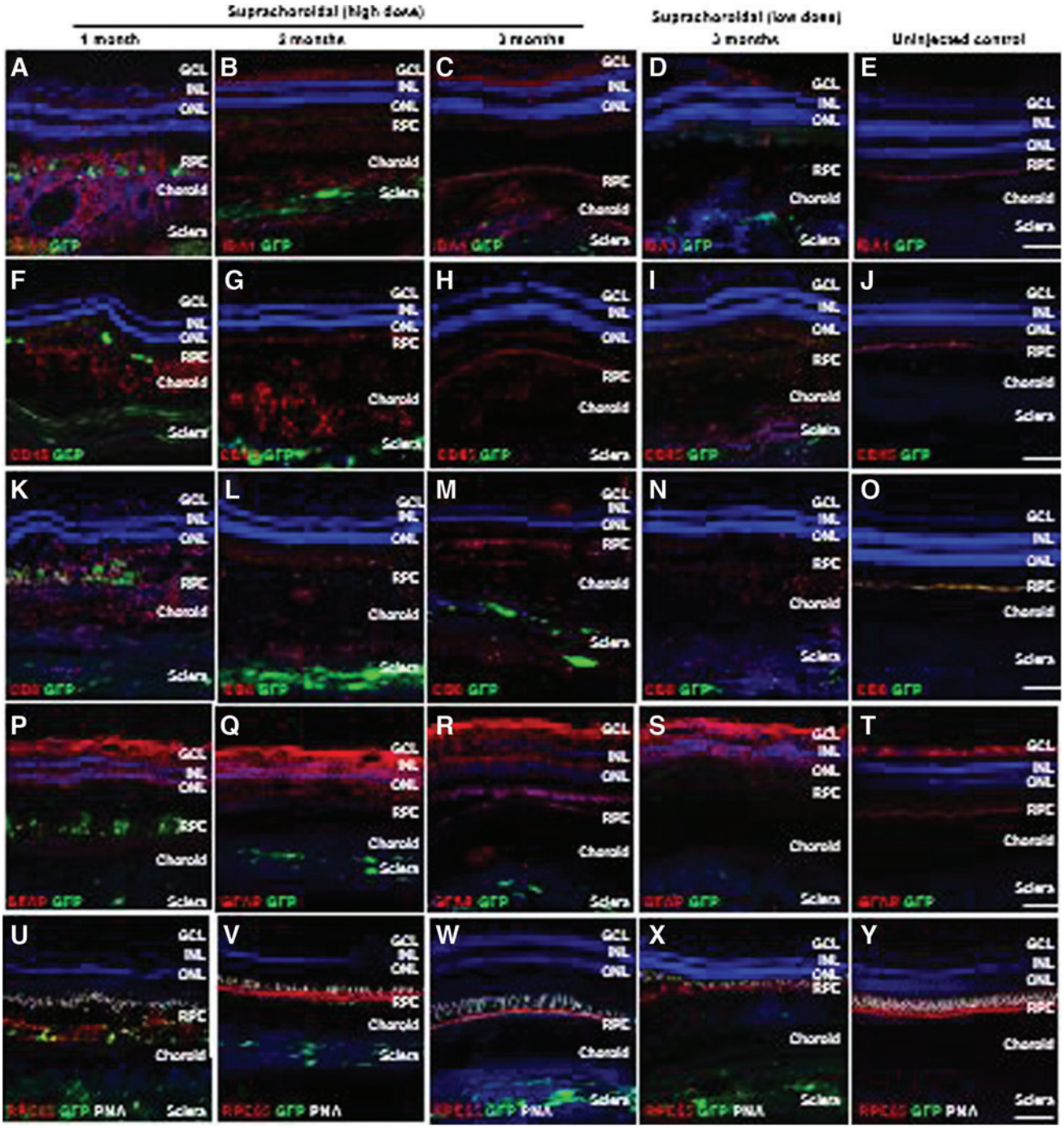

Figure 2. Local immune cell infiltration after suprachoroidal delivery of AAV8 in NHP eyes. **(A–Y)** Confocal fluorescence images of GFP transgene expression (*green*) co-immunostained with antibodies to IBA-1+ microglial cells **(A–E)**, CD45+ leukocytes **(F–J)**, CD8+ cytotoxic T cells **(K–O)**, and GFAP+ reactive gliosis **(P–T)**, as well as RPE65 (*red*) to label RPE cells and PNA (*white*) to label cone photoreceptor inner/out segments, along with DAPI (*blue*) to label cell nuclei in eyes at 1 month **(A, F, K, P,** and **U)**, 2 months **(B, G, L, Q,** and **V)**, and 3 months **(C, H, M, R,** and **W)** after high-dose or low-dose **(D, I, N, S,** and **X)** suprachoroidal AAV8 injections, compared to uninjected control eyes **(E, J, O, T,** and **V)**. Scale bars: 100 μm. GCL, ganglion cell layers; GFAP, glial fibrillary acidic protein; IBA-1, ionized calcium-binding adaptor-1; INL, inner nuclear layer; ONL, outer nuclear layer; PNA, peanut agglutinin; RPE, retinal pigment epithelium. Color images are available online.

fellow eyes (Rhesus 03 and 04). These studies suggest that suprachoroidal AAV delivery may result in some systemic distribution to peripheral organs such as the spleen and liver, but at much lower amounts than intravitreal injections.

DISCUSSION

Despite the presence of ocular immune privilege, AAV-mediated gene delivery to the eye triggers host immune responses that may vary with AAV dose, serotype, route of

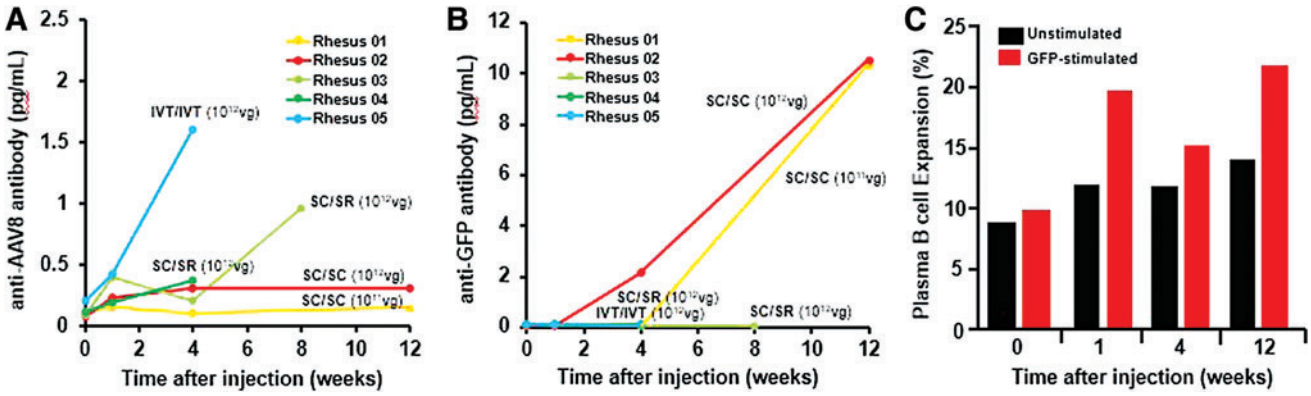

Figure 3. B cell-mediated humoral immune responses against AAV8 and GFP after suprachoroidal injections in NHP eyes. **(A, B)** *Line plots* compare serum anti-AAV8 antibody and anti-GFP antibody levels in rhesus macaques before and after bilateral suprachoroidal (SC/SC), suprachoroidal/subretinal (SC/SR), or bilateral intravitreal (IVT/IVT) AAV8 injections. **(C)** *Bar graphs* show flow cytometry analysis of plasma B cells with expansion upon GFP peptide stimulation from PBMCs collected at various time points after high-dose suprachoroidal AAV8 injections into both eyes in Rhesus 02. PBMC, peripheral blood mononuclear cell. Color images are available online.

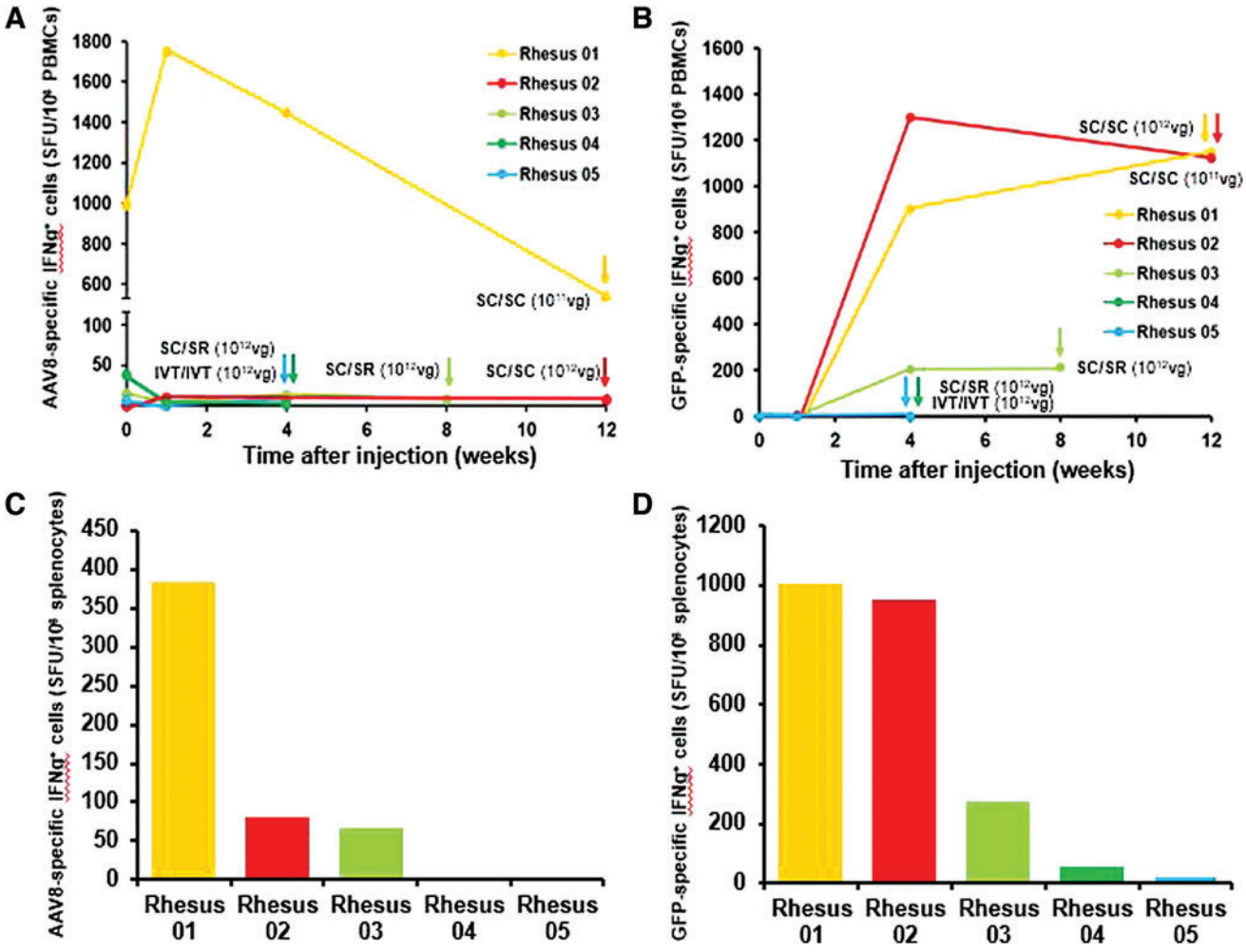

Figure 4. T cell-mediated immune responses against AAV8 and GFP after suprachoroidal injection. **(A, B)** Line plots compare IFN-γ-producing T cell response against AAV8 capsid and GFP transgene in PBMCs before and after bilateral suprachoroidal (SC/SC), suprachoroidal/subretinal (SC/SR), or bilateral intravitreal (IVT/IVT) AAV8 injections. **(C, D)** *Bar plots* compare IFN-γ-producing T cell response against AAV8 capsid and GFP transgene from splenocytes collected at necropsy, as indicated by the corresponding *colored arrows* for each animal. IFN-γ, interferon gamma; SC, suprachoroidal; SFU, spot-forming unit; SR, subretinal. Color images are available online.

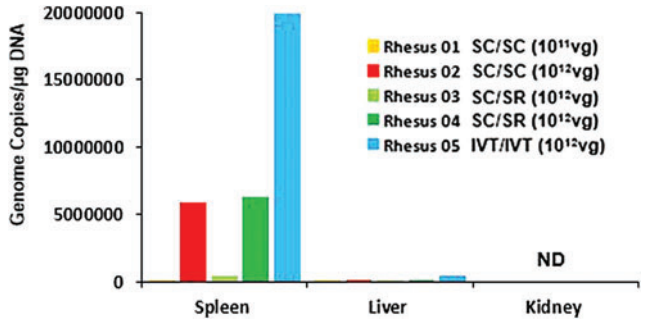

Figure 5. Systemic biodistribution of AAV8 after suprachoroidal injections. *Bar graphs* show quantification of virally encoded GFP genome copies measured from peripheral organs, including spleen, liver, and kidney, which were collected at the time of necropsy. IVT, intravitreal; ND, not detected. Color images are available online.

delivery, and type of transgene. Early studies from the RPE65 gene therapy trials using an AAV2 vector reported a dose-dependent immune response with intraocular inflammation observed in the high-dose (1×10^{12} vg/eye), but not low-dose (1×10^{11} vg/eye) patient cohorts.[1] The presence of pre-existing immunity also varies with AAV serotypes, as seroprevalence of anti-AAV2 NAbs in humans has been reported to range between 30% and 60%, while NAbs against AAV7, AAV8, and AAV9 are lower at 15–30%.[35,36] Importantly, the route of vector delivery is a major determinant of host immune responses. Intravitreal injections of AAV2 and AAV8 trigger more intraocular inflammation, with more robust humoral and cellular immune responses in mice and NHPs than subretinal delivery,[13,16,33,37,38] presumably due to the greater egress of viral particles into systemic circulation from the vitreous cavity.

In this ancillary analysis of a recent study, we evaluated host immune responses to a novel mode of delivering viral vectors into the suprachoroidal space of NHPs using transscleral microneedles.[21,22] Using an AAV8 vector to express GFP under a CMV promoter, we found that suprachoroidal delivery can trigger a peripheral chorioretinitis and vitritis with outer retinal disruption at month 1 after viral injection, but subsequently showed resolution of inflammation and restoration of retinal architecture at month 3, after systemic corticosteroid administration. We found that the inflammation was accompanied by both humoral and cell-mediated responses to the GFP transgene product, but a less pronounced humoral response to the AAV8 capsid than intravitreal injections.

The host immune responses to the GFP transgene and viral vector can be explained by the pattern of transgene expression, systemic biodistribution of the viral vectors, and unique location of the suprachoroidal space outside the blood–retinal barrier. The blood–retinal barrier is composed of an inner barrier that consists of retinal capillary endothelium, and an outer barrier formed by RPE tight junctions. While the vitreous cavity and subretinal space are immune-privileged ocular compartments within this barrier, the suprachoroidal space is adjacent to the highly fenestrated choroidal vasculature and readily interfaces with macrophages in the choroid and sclera outside of this barrier.

In contrast to intravitreal and subretinal injections, which enabled focal GFP transduction within the neurosensory retina, suprachoroidal AAV8 produced broad regions of transgene expression in the RPE and sclera, which are outside the blood–retinal barrier. RPE are potent antigen-presenting cells (APCs) of the retina,[39,40] while macrophages and dendritic cells are prevalent in the sclera.[41] In our study, we observed Iba1+ macrophages/microglia surrounding GFP-expressing RPE, but did not clearly detect any GFP-expressing Iba1+ cells. While the exact cell type responsible for antigen presentation is unclear, we found that GFP expression in the RPE after suprachoroidal AAV was transient, with loss of detectable expression by 2 months, possibly due to macrophage and cytotoxic T cell infiltration, which may contribute to the elimination of transduced cells. By contrast, suprachoroidal AAV-mediated GFP expression persisted in scleral fibroblasts through month 3, even in eyes that received a lower vector dose.

Our results suggest that immune sensitization likely occurs locally in the eye through scleral fibroblasts rather than in peripheral tissues, as both humoral and cellular immune responses to GFP appeared to correlate with the greater transgene expression in the sclera after suprachoroidal injections, regardless of AAV dose, rather than to the higher amounts of viral genomes in peripheral organs after intravitreal delivery. This hypothesis and our results are consistent with the study by Vandenberghe *et al.*,[42] in which T cell responses against GFP, but not AAV capsid were found in NHP eyes after subretinal AAV8 delivery.

Even though the suprachoroidal space is outside the blood–retinal barrier, intravitreal AAV8 triggered a more robust humoral response to the viral capsid, likely due to greater systemic exposure to the AAV8 vector as shown in our biodistribution studies. Trabecular outflow through the canal of Schlemm accounts for 80–90% of vitreous and aqueous humor drainage from the eye, while uveoscleral outflow, which likely mediates AAV egress from the suprachoroidal space, is less efficient.[43] Our findings are consistent with previous studies demonstrating greater humoral immune responses after intravitreal versus subretinal injections,[37,38,44] and suggest that the suprachoroidal space may have better retention of viral particles than the vitreous cavity.

Although this study focused on AAV8-binding antibodies, we previously found a similar pattern of NAb response that was also more pronounced after intravitreal than suprachoroidal AAV delivery.[21] NAbs prevent viral particles from phagocytosis by blocking essential receptor interactions between the virus and host cells, and may also sequester AAV distribution to the spleen.[45] By contrast, the role of non-NAbs is unclear, and may enhance the clearance of AAV

vectors through opsonization or have the opposite effects of Nabs.[45,46] Interestingly, although serum NAbs can impact the re-administration of AAV given intravitreally,[44] they do not appear to affect the functional effectiveness of AAV readministered subretinally.[47] Because a major advantage of suprachoroidal AAV delivery is the capacity for repeated injections, future studies are necessary to determine if the effectiveness of suprachoroidal AAV re-administration may be impacted on repeated dosing.

Our biodistribution assays demonstrated greater peripheral distribution of viral genomes to the spleen and liver after intravitreal injections, compared with suprachoroidal AAV8 delivery, similar to findings by Seitz *et al.* who also found more viral genomes in peripheral organs after intravitreal versus subretinal AAV8 in NHPs.[48] The higher expression in the spleen alludes to a deviant immune response similar to anterior chamber-associated immune deviation—a phenomenon in which immunogen bearing APCs from the eye migrate through the trabecular meshwork to the spleen, where afferent CD4+ Th1 cells and efferent CD8+ cytotoxic T cells differentiate and mature.[15] Further studies to distinguish more proinflammatory from immunosuppressive T cell subtypes could elucidate the nature of the host cellular immune responses, and help refine strategies for mitigation. The timing of T cell-directed immunosuppression, for example, has been shown to impact transgene immunogenicity after subretinal AAV delivery.

There are several limitations to our study. Like humans, rhesus macaques are native hosts of AAVs without significant disease association,[49,50] but exhibit higher seroprevalence of pre-existing immunity to AAV8 capsids.[51,52] Although we prescreened animals for the absence of NAbs against AAV8, one animal in our study was found to have a pre-existing T cell response, even though immune studies in liver-directed gene therapy indicate that memory T cells to AAV capsids are likely to be infrequent in humans and do not eliminate AAV-transduced hepatocytes.[53] Also, the AAV vectors in our study were not generated under Good Manufacturing Practice conditions, and may exhibit greater immunogenicity. In addition, although NHPs are excellent preclinical models due to their similar ocular anatomy and immune responses, they do not mount the same level of AAV-specific T cell responses as humans in liver-directed gene transfer,[53] possibly due to differences in AAV life cycles between humans and NHPs, more efficient recruitment of primed human T cells to the liver,[54–56] or loss of inhibitory sialic acid-recognizing Ig superfamily lectins on human T cells.

Also, we are limited by the number of animals in this study, with only one animal that received intravitreal injections, and the need to sacrifice some animals at earlier time points due to the loss of GFP expression (*e.g.*, Rhesus 03 and 04); we cannot determine the host immune responses from these animals at later time points. Finally, because two animals in our study also had subretinal AAV injections in their contralateral eyes, their immune responses may not fully reflect the consequences of suprachoroidal delivery. However, as previous studies have shown that subretinal injections elicit minimal humoral or cellular responses,[13,38] we believe that the immune responses in these animals are more likely attributable to the suprachoroidal injections.

In summary, our study indicates that the suprachoroidal space has significant potential as a novel route for viral-mediated ocular gene therapy. A prior study reported by Ding *et al.* also demonstrated effective AAV8-mediated gene transfer after suprachoroidal delivery in rats, a pig, and three rhesus macaques, with a more diffuse and broader pattern of transgene expression than those in our studies. In addition, Han *et al.* compared transduction efficiency of several AAV serotypes in the rat retina and found that suprachoroidal injections resulted in wider spread of virus compared with subretinal injection.[57]

These prior studies relied mostly on rodents in which the anatomy of the suprachoroidal space differs from humans and other primate species. Also, we employed a higher viral titer (7×10^{12} vs. 4.75×10^{11} vs. 5×10^{10}), and importantly, used transscleral microneedles that have been validated and utilized in human clinical trials (NCT02949024, NCT02303184, and NCT03097315) compared to the conventional 27-gauge needles or Hamilton cannulas employed by the other study using a free-hand technique, which may not be as reliable in accessing the microscopic potential space of the suprachoroid. The sensitivity for GFP detection may also differ between the use of *in vivo* SLO imaging and cross-sectional histology in our study, versus the flat-mounted histology in the other NHP study. Nevertheless, Ding *et al.* also demonstrated successful suprachoroidal delivery of an AAV8 vector expressing a more clinically relevant monoclonal antibody fragment to neutralize vascular endothelial growth factor (RGX-314).

Suprachoroidal injection of RGX-314 is currently under evaluation in human clinical trials for treatment of neovascular age-related macular degeneration. Neovascular retinal conditions that require gene therapies that employ a biofactory approach may be uniquely suited for suprachoroidal delivery, in contrast to inherited retinal conditions caused by mutations in retinal cells such as photoreceptors and RPE. Also, unlike the GFP transgene in our study, which is a known immunogen and not native to primate species,[58] these trials employ human-based transgenes and are less likely to generate as robust an immune response. Our study also employed a CMV promoter, which has been associated with ocular toxicity, not otherwise observed using photoreceptor-specific promoters for AAV transgene expression.[59] Future studies that employ human-derived and more clinically relevant promoters and transgenes could better predict host immune responses after suprachoroidal AAV injections. For example, using cell-specific promoters that minimize expression in the sclera

could reduce the risk of triggering host immune responses. Such studies will help facilitate clinical translation of suprachoroidal vector delivery for retinal gene therapy.

ACKNOWLEDGMENTS

We thank Marie Burns and Huaiyang Chen for AAV production, Amanda Carpenter for PBMC and splenocyte preparation, Jeffrey Roberts and John Morrison for CNPRC logistics, Monica Motta for assistance with animal imaging, and Dennis Hartigan-O'Connor for discussions. We also thank Clearside Biomedical and Glenn Noronha, Jesse Yoo, and Donna Taraborelli for providing the suprachoroidal microneedles used in our study.

AUTHORS' CONTRIBUTIONS

G.Y. conceived the study design, obtained funding, performed the examinations, intraocular injections, and *in vivo* imaging, and supervised the study. S.H.C., T.-N.S., and T.N. conducted the binding antibody assays, ELIspot assays, biodistribution studies, and immunohistochemistry. I.N.M. assisted clinical examination, injections, and tissue collection. A.M. conducted flow cytometry and analyzed data. G.Y. and S.H.C. analyzed all data and wrote the article. G.Y., S.H.C., T.C., P.S. and S.M.T. critically reviewed the article.

DISCLAIMER

The content is solely the responsibility of the authors and does not necessarily represent the official views of the funding agencies.

AUTHOR DISCLOSURE

G.Y. received research support from Clearside Biomedical, Genentech, and Iridex, and personal fees for consultancy from Alimera, Allergan, Carl Zeiss Meditec, Clearside Biomedical, Genentech, Gyroscope Therapeutics, Intergalactic Therapeutics, Iridex, Regeneron, Topcon, and Verily. T.C. is an employee with and has equity ownership in Clearside Biomedical. Transscleral microneedles used in this study were provided by Clearside Biomedical, and may be requested under Material Transfer Agreement (MTA).

FUNDING INFORMATION

This study was supported by the California National Primate Research Center pilot grant program and base grant NIH P510D011107. G.Y. is supported by NIH K08 EY026101, NIH R21 EY031108, and Macula Society. S.M.T. is supported by U24 U24EY029904. The AAV8 vector was produced by the Center for Vision Sciences Molecular Constructs and Packaging core facility supported by NIH P30 EY012576. No funding organization had any role in the design or conduct of this research.

SUPPLEMENTARY MATERIAL

Supplementary Figure S1
Supplementary Table S1

REFERENCES

1. Bainbridge JW, Mehat MS, Sundaram V, et al. Long-term effect of gene therapy on Leber's congenital amaurosis. N Engl J Med 2015;372:1887–1897.
2. Bainbridge JW, Smith AJ, Barker SS, et al. Effect of gene therapy on visual function in Leber's congenital amaurosis. N Engl J Med 2008;358:2231–2239.
3. Maguire AM, Simonelli F, Pierce EA, et al. Safety and efficacy of gene transfer for Leber's congenital amaurosis. N Engl J Med 2008;358:2240–2248.
4. Maguire AM, High KA, Auricchio A, et al. Age-dependent effects of RPE65 gene therapy for Leber's congenital amaurosis: a phase 1 dose-escalation trial. Lancet 2009;374:1597–1605.
5. Cideciyan AV, Hauswirth WW, Aleman TS, et al. Vision 1 year after gene therapy for Leber's congenital amaurosis. N Engl J Med 2009;361:725–727.
6. Hauswirth WW, Aleman TS, Kaushal S, et al. Treatment of leber congenital amaurosis due to RPE65 mutations by ocular subretinal injection of adeno-associated virus gene vector: short-term results of a phase I trial. Hum Gene Ther 2008;19:979–990.
7. Wang D, Tai PWL, Gao G. Adeno-associated virus vector as a platform for gene therapy delivery. Nat Rev Drug Discov 2019;18:358–378.
8. Manno CS, Pierce GF, Arruda VR, et al. Successful transduction of liver in hemophilia by AAV-Factor IX and limitations imposed by the host immune response. Nat Med 2006;12:342–347.
9. Wang Z, Allen JM, Riddell SR, et al. Immunity to adeno-associated virus-mediated gene transfer in a random-bred canine model of Duchenne muscular dystrophy. Hum Gene Ther 2007;18:18–26.
10. Halbert CL, Standaert TA, Aitken ML, et al. Transduction by adeno-associated virus vectors in the rabbit airway: efficiency, persistence, and readministration. J Virol 1997;71:5932–5941.
11. Kessler PD, Podsakoff GM, Chen X, et al. Gene delivery to skeletal muscle results in sustained expression and systemic delivery of a therapeutic protein. Proc Natl Acad Sci U S A 1996;93:14082–14087.
12. Xiao W, Chirmule N, Schnell MA, et al. Route of administration determines induction of T-cell-independent humoral responses to adeno-associated virus vectors. Mol Ther 2000;1:323–329.
13. Li Q, Miller R, Han PY, et al. Intraocular route of AAV2 vector administration defines humoral immune response and therapeutic potential. Mol Vis 2008;14:1760–1769.
14. Shirley JL, de Jong YP, Terhorst C, et al. Immune responses to viral gene therapy vectors. Mol Ther 2020;28:709–722.
15. Streilein JW. Ocular immune privilege: therapeutic opportunities from an experiment of nature. Nat Rev Immunol 2003;3:879–889.
16. Barker SE, Broderick CA, Robbie SJ, et al. Subretinal delivery of adeno-associated virus serotype 2 results in minimal immune responses that allow

repeat vector administration in immunocompetent mice. J Gene Med 2009;11:486–497.

17. Bennett J, Ashtari M, Wellman J, et al. AAV2 gene therapy readministration in three adults with congenital blindness. Sci Transl Med 2012;4:120ra115.
18. Dalkara D, Byrne LC, Klimczak RR, et al. In vivo-directed evolution of a new adeno-associated virus for therapeutic outer retinal gene delivery from the vitreous. Sci Transl Med 2013;5:189ra176.
19. Petrs-Silva H, Dinculescu A, Li Q, et al. Novel properties of tyrosine-mutant AAV2 vectors in the mouse retina. Mol Ther 2011;19:293–301.
20. Lukason M, DuFresne E, Rubin H, et al. Inhibition of choroidal neovascularization in a nonhuman primate model by intravitreal administration of an AAV2 vector expressing a novel anti-VEGF molecule. Mol Ther 2011;19:260–265.
21. Yiu G, Chung SH, Mollhoff IN, et al. Suprachoroidal and subretinal injections of AAV using transscleral microneedles for retinal gene delivery in nonhuman primates. Mol Ther Methods Clin Dev 2020;16:179–191.
22. Ding K, Shen J, Hafiz Z, et al. AAV8-vectored suprachoroidal gene transfer produces widespread ocular transgene expression. J Clin Invest 2019;129:4901–4911.
23. Yiu G, Pecen P, Sarin N, et al. Characterization of the choroid-scleral junction and suprachoroidal layer in healthy individuals on enhanced-depth imaging optical coherence tomography. JAMA Ophthalmol 2014;132:174–181.
24. Emami-Naeini P, Yiu G. Medical and surgical applications for the suprachoroidal space. Int Ophthalmol Clin 2019;59:195–207.
25. Willoughby AS, Vuong VS, Cunefare D, et al. Choroidal changes after suprachoroidal injection of triamcinolone acetonide in eyes with macular edema secondary to retinal vein occlusion. Am J Ophthalmol 2018;186:144–151.
26. Lampen SIR, Khurana RN, Noronha G, et al. Suprachoroidal space alterations following delivery of triamcinolone acetonide: post-hoc analysis of the Phase 1/2 HULK Study of Patients with diabetic macular edema. Ophthalmic Surg Lasers Imaging Retina 2018;49:692–697.
27. Kim YC, Edelhauser HF, Prausnitz MR. Targeted delivery of antiglaucoma drugs to the supraciliary space using microneedles. Invest Ophthalmol Vis Sci 2014;55:7387–7397.
28. Olsen TW, Feng X, Wabner K, et al. Cannulation of the suprachoroidal space: a novel drug delivery methodology to the posterior segment. Am J Ophthalmol 2006;142:777–787.
29. Olsen TW, Feng X, Wabner K, et al. Pharmacokinetics of pars plana intravitreal injections versus microcannula suprachoroidal injections of bevacizumab in a porcine model. Invest Ophthalmol Vis Sci 2011;52:4749–4756.
30. Patel SR, Berezovsky DE, McCarey BE, et al. Targeted administration into the suprachoroidal space using a microneedle for drug delivery to the posterior segment of the eye. Invest Ophthalmol Vis Sci 2012;53:4433–4441.
31. Patel SR, Lin AS, Edelhauser HF, et al. Suprachoroidal drug delivery to the back of the eye using hollow microneedles. Pharm Res 2011;28:166–176.
32. Yeh S, Khurana RN, Shah M, et al. Efficacy and safety of suprachoroidal CLS-TA for macular edema secondary to noninfectious uveitis: Phase 3 Randomized Trial. Ophthalmology 2020;127:948–955.
33. Reichel FF, Dauletbekov DL, Klein R, et al. AAV8 can induce innate and adaptive immune response in the primate eye. Mol Ther 2017;25:2648–2660.
34. Yiu G, Vuong VS, Oltjen S, et al. Effect of uveal melanocytes on choroidal morphology in rhesus macaques and humans on enhanced-depth imaging optical coherence tomography. Invest Ophthalmol Vis Sci 2016;57:5764–5771.
35. Vandamme C, Adjali O, Mingozzi F. Unraveling the complex story of immune responses to AAV vectors trial after trial. Hum Gene Ther 2017;28:1061–1074.
36. Calcedo R, Vandenberghe LH, Gao G, et al. Worldwide epidemiology of neutralizing antibodies to adeno-associated viruses. J Infect Dis 2009;199:381–390.
37. Maclachlan TK, Lukason M, Collins M, et al. Preclinical safety evaluation of AAV2-sFLT01- a gene therapy for age-related macular degeneration. Mol Ther 2011;19:326–334.
38. Reichel FF, Peters T, Wilhelm B, et al. Humoral immune response after intravitreal but not after subretinal AAV8 in primates and patients. Invest Ophthalmol Vis Sci 2018;59:1910–1915.
39. Osusky R, Dorio RJ, Arora YK, et al. MHC class II positive retinal pigment epithelial (RPE) cells can function as antigen-presenting cells for microbial superantigen. Ocul Immunol Inflamm 1997;5:43–50.
40. Lipski DA, Dewispelaere R, Foucart V, et al. MHC class II expression and potential antigen-presenting cells in the retina during experimental autoimmune uveitis. J Neuroinflammation 2017;14:136.
41. Schlereth SL, Kremers S, Schrodl F, et al. Characterization of antigen-presenting macrophages and dendritic cells in the healthy human sclera. Invest Ophthalmol Vis Sci 2016;57:4878–4885.
42. Vandenberghe LH, Bell P, Maguire AM, et al. Dosage thresholds for AAV2 and AAV8 photoreceptor gene therapy in monkey. Sci Transl Med 2011;3:88ra54.
43. Karpinich NO, Caron KM. Schlemm's canal: more than meets the eye, lymphatics in disguise. J Clin Invest 2014;124:3701–3703.
44. Kotterman MA, Yin L, Strazzeri JM, et al. Antibody neutralization poses a barrier to intravitreal adeno-associated viral vector gene delivery to non-human primates. Gene Ther 2015;22:116–126.
45. Wang L, Calcedo R, Bell P, et al. Impact of pre-existing immunity on gene transfer to nonhuman primate liver with adeno-associated virus 8 vectors. Hum Gene Ther 2011;22:1389–1401.
46. Fitzpatrick Z, Leborgne C, Barbon E, et al. Influence of pre-existing anti-capsid neutralizing and binding antibodies on AAV vector transduction. Mol Ther Methods Clin Dev 2018;9:119–129.
47. Amado D, Mingozzi F, Hui D, et al. Safety and efficacy of subretinal readministration of a viral vector in large animals to treat congenital blindness. Sci Transl Med 2010;2:21ra16.
48. Seitz IP, Michalakis S, Wilhelm B, et al. Superior retinal gene transfer and biodistribution profile of subretinal versus intravitreal delivery of AAV8 in nonhuman primates. Invest Ophthalmol Vis Sci 2017;58:5792–5801.
49. Calcedo R, Wilson JM. Humoral immune response to AAV. Front Immunol 2013;4:341.
50. Boutin S, Monteilhet V, Veron P, et al. Prevalence of serum IgG and neutralizing factors against adeno-associated virus (AAV) types 1, 2, 5, 6, 8, and 9 in the healthy population: implications for gene therapy using AAV vectors. Hum Gene Ther 2010;21:704–712.
51. Gao G, Alvira MR, Somanathan S, et al. Adeno-associated viruses undergo substantial evolution in primates during natural infections. Proc Natl Acad Sci U S A 2003;100:6081–6086.
52. Calcedo R, Morizono H, Wang L, et al. Adeno-associated virus antibody profiles in newborns, children, and adolescents. Clin Vaccine Immunol 2011;18:1586–1588.
53. Li H, Murphy SL, Giles-Davis W, et al. Pre-existing AAV capsid-specific CD8+ T cells are unable to eliminate AAV-transduced hepatocytes. Mol Ther 2007;15:792–800.
54. Guidotti LG, Iannacone M. Effector CD8 T cell trafficking within the liver. Mol Immunol 2013;55:94–99.
55. Lang KS, Georgiev P, Recher M, et al. Immunoprivileged status of the liver is controlled by toll-like receptor 3 signaling. J Clin Invest 2006;116:2456–2463.
56. Nguyen DH, Hurtado-Ziola N, Gagneux P, et al. Loss of Siglec expression on T lymphocytes during human evolution. Proc Natl Acad Sci U S A 2006;103:7765–7770.
57. Han IC, Cheng JL, Burnight ER, et al. Retinal tropism and transduction of adeno-associated virus varies by serotype and route of delivery (intravitreal, subretinal, or suprachoroidal) in rats. Hum Gene Ther 2020;31:1288–1299.
58. Ansari AM, Ahmed AK, Matsangos AE, et al. Cellular GFP toxicity and immunogenicity: potential confounders in in vivo cell tracking experiments. Stem Cell Rev Rep 2016;12:553–559.
59. Huang X, Zhou G, Wu W, et al. Genome editing abrogates angiogenesis in vivo. Nat Commun 2017;8:112.

Received for publication October 19, 2020;
accepted after revision December 22, 2020.

Published online: January 14, 2021.